

# Study of Mechanism for Hexane Decomposition with Gliding Arc Gas Discharge

J. H. Yan · Zh. Bo · X. D. Li · Ch. M. Du ·  
K. F. Cen · B. G. Chéron

Received: 18 May 2006 / Accepted: 27 July 2006 / Published online: 8 March 2007  
© Springer Science+Business Media, LLC 2007

**Abstract** The mechanism of hexane decomposition under gliding arc gas discharge conditions is studied from both qualitative and quantitative analyses of its products for various hexane initial concentrations and different background atmospheres : nitrogen, argon, air (O<sub>2</sub> 21% N<sub>2</sub> 79% vol.) and N<sub>2</sub>–O<sub>2</sub> mixtures. The decomposition rate, which decreases with increasing hexane initial concentration, can reach 94% when the carrier gas is air. Due to the electron energy consumed by the dissociation of nitrogen, the decomposition rate of hexane in nitrogen is lower than in argon. The radical channel plays a predominant role in the hexane decomposition process. With increasing oxygen concentration in the carrier gas, the hexane decomposition rate increases and promotes the conversion of CO–CO<sub>2</sub>, but it also leads to the formation of NO<sub>2</sub>.

**Keywords** Gliding arc gas discharge · Hexane · Decomposition products · Plasma

## 1 Introduction

Volatile organic compounds (VOCs) are particularly burdensome for the natural environment. Most of them are harmful to human health while some are responsible for the greenhouse effect. Removal of these toxic species becomes an important task in achieving environmentally accepted pollutants levels. However, applications of conventional technologies for VOCs removal process, as thermal and catalytic incinerations, activated carbon adsorption and condensation, are limited owing to their own disadvantages. As an alternative, many studies devoted to VOCs

---

J. H. Yan (✉) · Zh. Bo · X. D. Li · Ch. M. Du · K. F. Cen  
State Key laboratory of Clean Energy Utilization, Institute for Thermal Power Engineering,  
Zhejiang University, Hangzhou 310027, P.R. China  
e-mail: yanjh@cmee.zju.edu.cn

B. G. Chéron  
UMR 6614(CORIA), University of Rouen, 76821 Mont Saint Aignan, Rouen, France

destruction by atmospheric non-thermal plasma are conducted since the last 10 years [1–4] by using electron-beam irradiation and various electrical discharge systems. As compared with traditional control methods, the non-thermal plasma technology has demonstrated its technical and economical feasibility for VOCs abatement.

The gliding arc discharge (GA) is an auto-oscillating phenomenon which develops between at least two electrodes that are immersed in a laminar or turbulent gas flow. In the 0.5–5 atm pressure range, GA devices produce high level power consecutive plasmas [5–8] which can directly process different gases. Many experimental studies have shown that the electron temperature (approximately 10 kK) in the GA discharges is much higher than the gas temperature (0.8–2.1 kK): in other words, the plasma is significantly in a non-equilibrium state [9–11]. In the early 1990's, GA devices have been developed by Czernichowski as an innovative approach to the solution of VOCs problem [12]. Nowadays, the potential of GA to decompose VOCs is clearly demonstrated: Krawczyk [13, 14] has applied GA to the treatment of tetrachloromethane and trichloromethane, with a conversion rate up to 90% and 100%. Czernichowski [15] has decomposed toluene and heptane by using GA, with a highest conversion rate in the 92% and 100% range. Our group has carried out researches on toluene and hexane decomposition by GA and we have obtained respectively 88% and 96% as highest conversion rate.

However, the VOCs decomposition mechanism and the chemical scheme of the byproducts formation in GA are not yet fully understood. Most of papers devoted to the decomposition of these molecules by using other various plasma technologies—such as dielectric barrier discharge, pulsed corona, and electron beam—suggest that the generation of energetic electrons is at once the initial step of the process and the source of various ions and radicals, [16–18] but the further chemical steps are complex and difficult to understand. Three main ways for VOCs decomposition are generally pointed out under non-thermal plasma conditions:

- (i) Dissociation of VOCs molecules by energetic electron impact
- (ii) Reactions between VOCs molecules and ions
- (iii) Reactions between VOCs molecules and radicals

Mok [16] mentioned that OH radicals are mainly produced through the neutral channel in corona discharge whereas this occurs through the ion channel under electron beam irradiation. Futamura [17] pointed that the radical mechanism governs VOCs decomposition in a dielectric barrier discharge reactor. The electron energetic level in gliding arc discharges (GA) (1–5 eV) is lower than that of dielectric barrier discharge (4–5 eV), corona discharge (5–10 eV) and electron beam (300–750 keV). Therefore significant differences in the nature and density of the produced ions and radicals may be expected when treating VOCs by a GA in comparison with the other reactors.

Our experimental study investigates the effects of both initial hexane concentration and background gas nature on the decomposition of the hexane when treated by a gliding arc discharge. Nitrogen, argon, air (O<sub>2</sub> 21% N<sub>2</sub> 79% vol.) and N<sub>2</sub>–O<sub>2</sub> mixture with different O<sub>2</sub> concentration are successively chosen as carrier gases; the role of the oxygen concentration in the hexane plasma decomposition process is also discussed. A realistic mechanism for the VOCs decomposition is derived from the analysis of its by-products in various physical conditions. This experimental study

also yields results which could be used in the purpose of establishing a theoretical model for the VOCs decomposition under GA conditions.

## 2 Experimental

### 2.1 Apparatus and procedures

Experiments are carried out by using a laboratory scale gliding arc discharge reactor at atmospheric pressure. The experimental setup, shown in Fig. 1, consists of a gas feed delivery system, a GA reactor and its power supply, and an analysis system.

The gas to be treated results from the mixing of a hexane flow with a carrier gas flow (argon, nitrogen, air or  $N_2$ – $O_2$  mixture). The concentration of hexane is controlled by means of mass flowmeters. The total flow rate is maintained at a fixed value: 11.7 Sl/min. The gas enters the GA reactor after passing through a drying column packed with a silica-gel desiccant. The GA reactor is supplied with a high voltage transformer (220 V/10 kV). In the purpose of measuring the composition of the gas flow, the flue is equipped with sample tubes which are set above and below the reactor.

### 2.2 Reactor and GA phenomenon

The GA reactor is displayed on Fig. 2: it mainly consists of two 96 mm long, 26 mm wide and 4 mm thick knife-shaped electrodes fixed on a teflon bed plate, a 1.5 mm in diameter gas nozzle and a teflon seal. The smallest distance between the electrodes is equal to 3 mm.

The GA phenomenon starts at the shortest gap between the electrodes by an initial breakdown of the gas to be processed. Then during few milliseconds the arc is pushed by the flow along the electrodes until the rupture of the ionized column. This event is followed by a new breakdown at the electrode throat and the cycle repeats as long as the voltage delivered by the transformer is high enough [8].

The experimental conditions are displayed in Table I.

### 2.3 Analytical methods

$C_6H_{14}$  (hexane),  $NO_x$ , CO and  $CO_2$  concentrations are quantified by means of a NICOLET NEXUS 670 Fourier Transform Infrared (FTIR) spectroscopy equipped

**Fig. 1** Schematic diagram of the experiment

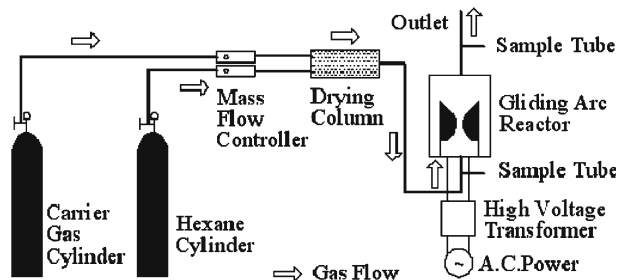


**Fig. 2** Gliding arc discharge reactor

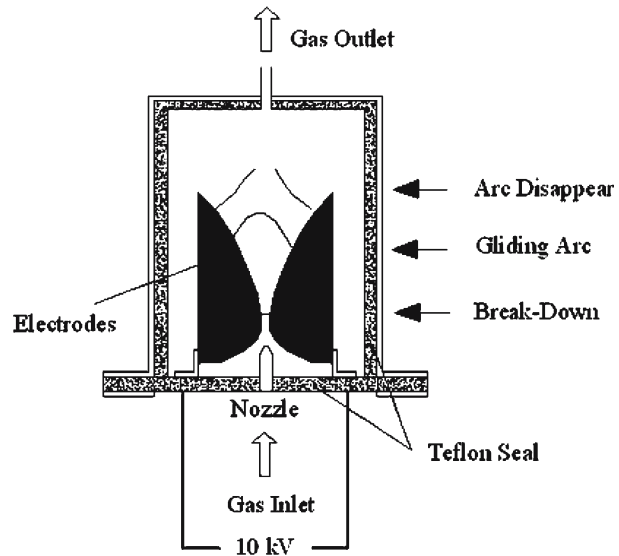


**Table 1** Experimental conditions

Variable (unit)	Value
Supply voltage (kV)	10
Supply frequency (Hz)	50
Total gas flow rate (Sl/min)	11.7
Hexane cylinder flow rate (Sl/min)	2.8–7.4
Carrier gas cylinder flow rate (Sl/min)	8.9–4.3

with a DTGs KBr detector. The spectral resolution is  $4 \text{ cm}^{-1}$  and every measurement is repeated four times. The temperature of sample cell is maintained at  $180^\circ\text{C}$ . The degradation by-products are detected and analyzed by using this FTIR system and a TRACE Gas Chromatograph with a flame ionization detector.

### 3 Results

We define the hexane decomposition rate  $\eta$  as the ratio of the hexane decomposition capacity :  $\Delta X = (X_0 - X)$ , to its initial concentration  $X_0$ , i.e.  $\eta = (X_0 - X)/X_0 \times 100\%$ , where  $X$  is its final concentration.

#### 3.1 Influence of the initial hexane concentration of the decomposition efficiency

Experiments are carried out in an atmospheric gliding arc discharge reactor. The initial hexane concentration can be adjusted by controlling both carrier gas and hexane flow rates. Seven measurements, which correspond to  $X_0 = 366, 458, 562, 667, 772, 876$  and  $968$  ppm are performed with the air as carrier gas.

The results are displayed on Figs. 3 and 4. The decomposition rate clearly decreases from about 95% to 82% when the hexane initial concentration is increased

**Fig. 3** Effect of initial concentration of hexane on the hexane decomposition rate

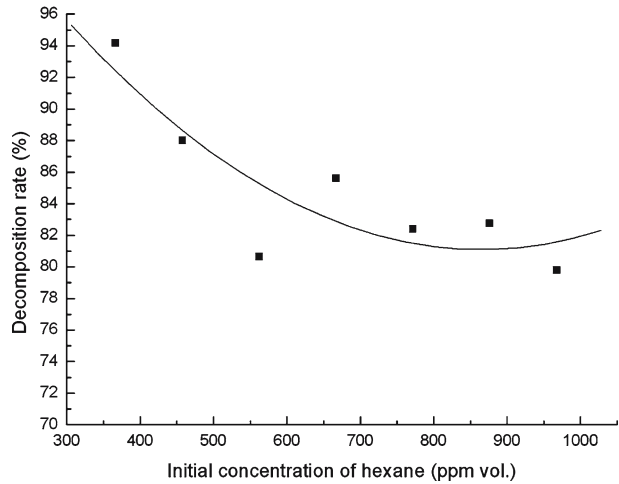
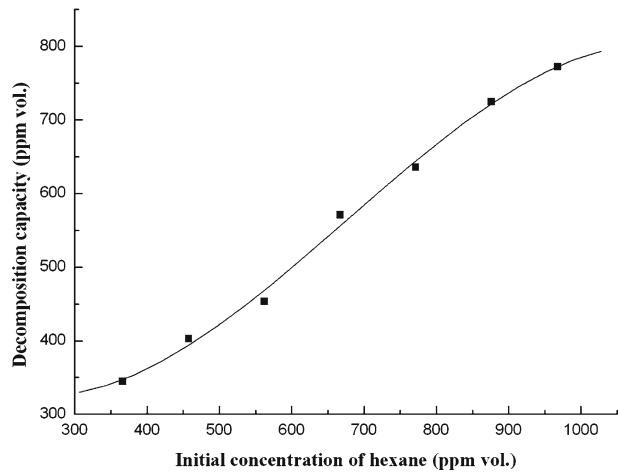


**Fig. 4** Effect of initial concentration of hexane on the hexane decomposition capacity

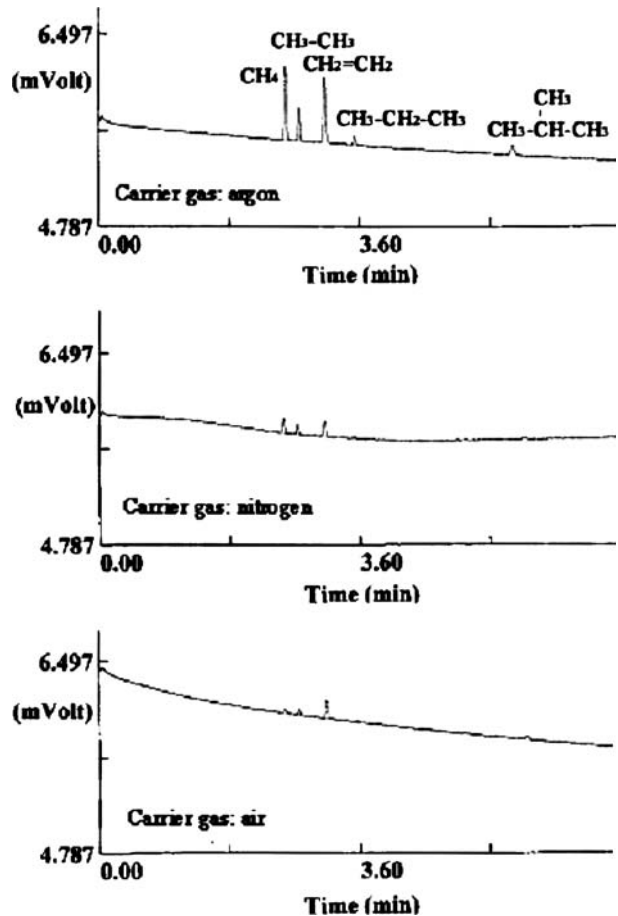


in the 350–700 ppm range. Then it is roughly constant. Consequently the decomposition capacity can be considered as a linear function of  $X_0$  over 700 ppm.

### 3.2 Analysis of hexane treatment by-products under argon, nitrogen and air atmosphere

In this section, we analyze the influence of the carrier gas (argon, nitrogen or air) on the nature and quantity of the decomposition by-products obtained for  $X_0 = 876$  ppm. Fig. 5 shows the hydrocarbons from  $C_1$  to  $C_4$  among the decomposition products detected by the TRACE GC. Methane  $CH_4$ , ethane  $C_2H_6$  and ethylene  $C_2H_4$  are the predominant compounds. A small amount of propane  $C_3H_8$  and isobutane  $C_4H_{10}$  is also identified. The concentration of these compounds is clearly higher in argon ( $CH_4$ : 888 ppm,  $C_2H_6$ : 112 ppm,  $C_2H_4$ : 259 ppm,  $C_3H_8$ : 25 ppm) than in nitrogen ( $CH_4$ : 44 ppm,  $C_2H_6$ : 28 ppm,  $C_2H_4$ : 15 ppm,  $C_3H_8$ : 0 ppm) or in air ( $CH_4$ : 17 ppm,  $C_2H_6$ : 57 ppm,  $C_2H_4$ : 12 ppm,  $C_3H_8$ : 0 ppm) atmosphere.

**Fig. 5** C<sub>1</sub>–C<sub>4</sub> hydrocarbons by-products obtained from hexane decomposition in nitrogen, argon and air (GC)



The FTIR absorption spectra of hexane decomposition products are displayed on Fig. 6. Acetylene C<sub>2</sub>H<sub>2</sub> (3373.9–3165.2 cm<sup>-1</sup> and 834.7–626.087 cm<sup>-1</sup>), methane CH<sub>4</sub> (3213.1–2986.9 cm<sup>-1</sup> and 1404.3–1182.6 cm<sup>-1</sup>), ethylene C<sub>2</sub>H<sub>4</sub> (1113.1–832.5 cm<sup>-1</sup>) are the main by-products when working under either argon or nitrogen atmosphere. Small amounts of carbon dioxide CO<sub>2</sub> (2330.8–2277.7 cm<sup>-1</sup> and 3764.9–3521.4 cm<sup>-1</sup>) and carbon monoxide CO (2216.8–2047.3 cm<sup>-1</sup>) are also detected. In contrast, the FTIR reveals no hydrocarbon among the hexane decomposition by-products with air as carrier gas : in these operating conditions, NO<sub>2</sub> (1660.9–1521.7 cm<sup>-1</sup> and 2947.8–2839.1 cm<sup>-1</sup>), CO<sub>2</sub> (2330.8–2277.7 cm<sup>-1</sup> and 3764.9–3521.4 cm<sup>-1</sup>) and CO (2216.8–2047.3 cm<sup>-1</sup>) are the major compounds.

### 3.3 Background effect on hexane decomposition efficiency

Fig. 7 shows the effect of the background gas type (argon, nitrogen or air) on both decomposition rate  $\eta$  and capacity  $\Delta X$ , with different initial hexane concentrations (366 ppm–968 ppm). The efficiency of the treatment is clearly greater when the GA is working in air than when the carrier gas is either nitrogen or argon. So we focus

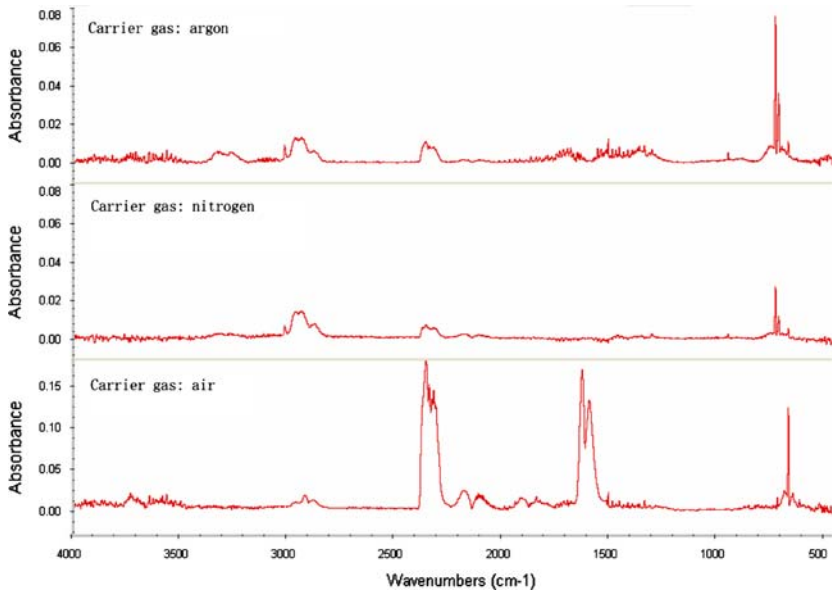


**Fig. 6** FTIR absorption spectra of decomposition products with argon, nitrogen and air as carrier gas

our attention, in the following, on the role played by oxygen in this chemical process developed under non-equilibrium plasma conditions.

### 3.4 Influence of oxygen concentration on the hexane decomposition

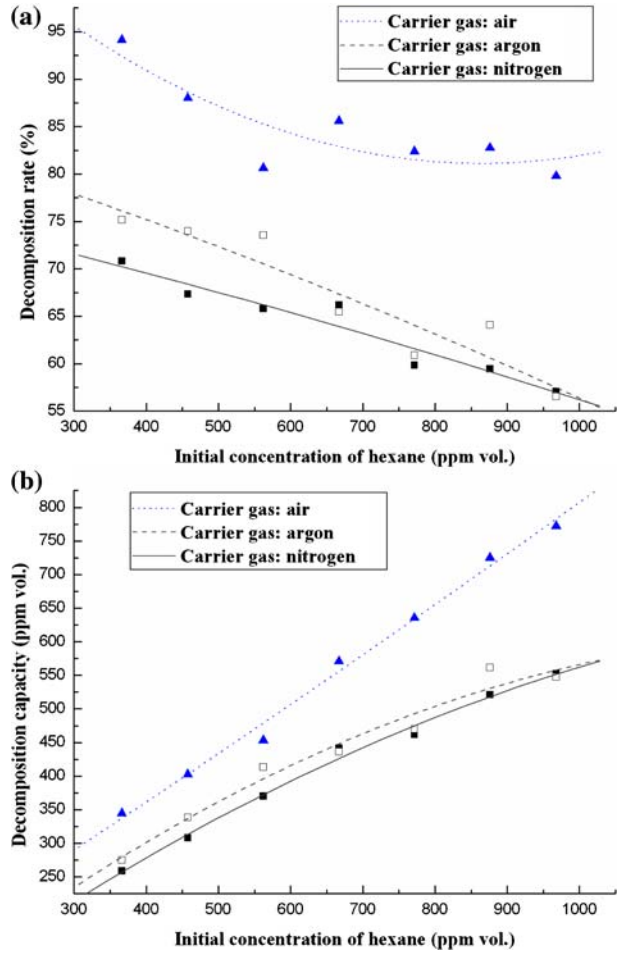
The hexane to be treated is carried into the GA reactor by a  $N_2$ – $O_2$  mixture with variable oxygen concentration (0, 2, 8, 11, 13, 15, 21% vol.). Its initial concentration is equal to  $X_0 = 876$  ppm. As shown on Fig. 8, the hexane decomposition is continuously increasing (from 59.5% to 82.8%) when the oxygen concentration in the carrier gas is increased. This effect is rather steep at low concentration (between 0 and 10%) and it seems to saturate when the oxygen concentration reaches its standard value in air (21%).

Fig. 9 shows that, among the decomposition products, the concentration of  $CO_2$ , CO, and  $NO_2$  are increasing with increasing  $O_2$  concentration in the carrier gas. When the oxygen concentration is lower than 2%, no  $NO_2$  formation is observed whereas the detected amounts of  $CO_2$  and CO remain quite small.

The variations of the  $CO_2$  selectivity defined as the ratio:  $S_{CO_2} = [CO_2]/([CO_2] + [CO])$  as a function of the  $O_2$  concentration are displayed in Table 2. The ratio of hexane which is transformed into CO and  $CO_2$  to the total decomposed hexane is continuously increasing from 0.1 to 0.9 when the  $O_2$  concentration varies between less than 2–15%. Most of the decomposed hexane is transformed into  $CO_2$  and CO when the  $O_2$  concentration is over 15%.

When considering the variations of the  $CO_2$  selectivity, two  $O_2$  concentration ranges can be distinguished : between 0 and 13%,  $S_{CO_2}$  is increasing from 0.477 to

**Fig. 7** Effect of background gas type on the hexane decomposition rate (a) and decomposition capacity (b) initial concentration varying in the 366–968 ppm range



**Fig. 8** Effect of oxygen concentration on the decomposition rate of hexane

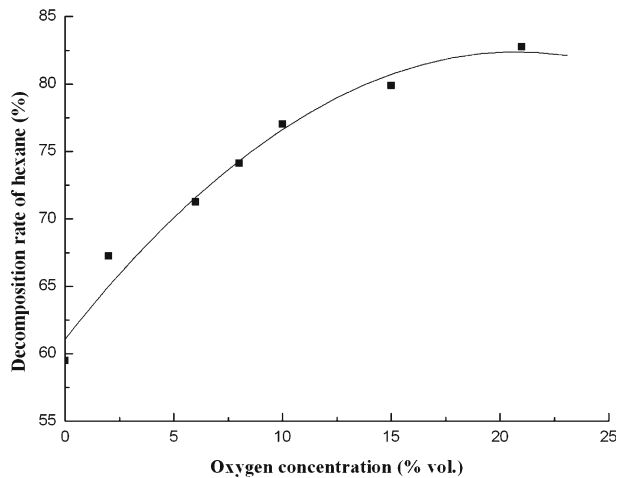
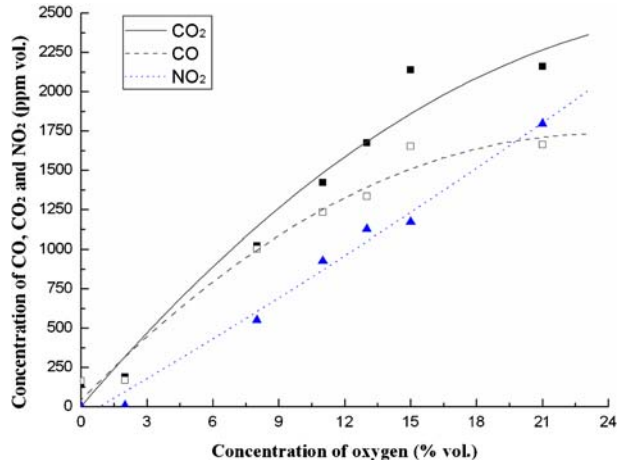




**Fig. 9** Effect of oxygen concentration on the CO<sub>2</sub>, CO and NO<sub>2</sub> formation



0.556, then its value is approximately constant, and equal to 0.56, between 13% and 21%.

These data show that the oxygen promotes the oxidation of CO to CO<sub>2</sub>.

#### 4 Discussion

On the basis of these experimental results, we suggest the following main reactions for the hexane decomposition process :

R1: Hexane dissociations by electron impact.

In a gliding arc, the mean energy of the free electrons (1–5 eV) is high enough to break the hexane C–C and C–H bonds, the energy of which are around 3–4 eV. As displayed on Fig. 10, the electron impacts on hexane molecule can lead to the creation of six different by-products.

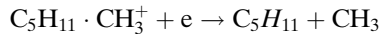
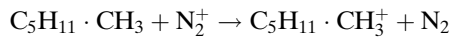
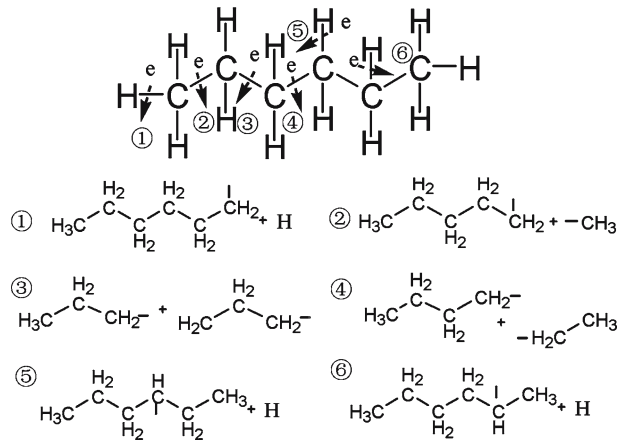
R2 : Reactions between ions and hexane.

After ionization of the carrier gas (N<sub>2</sub>, O<sub>2</sub> or Ar), the charge of N<sub>2</sub><sup>+</sup>, O<sub>2</sub><sup>+</sup> or Ar<sup>+</sup> is transferred to the hexane molecule. When recombining with a free electron, the ion products radicals through a dissociative process. For example

**Table 2** CO<sub>2</sub> selectivity as a function of oxygen concentration

Oxygen concentration (% vol.)	Hexane decomposition rate (%)	Conversion of hexane to CO <sub>2</sub> (%)	Conversion of hexane to CO (%)	Ratio of hexane transformed to CO and CO <sub>2</sub> to the total decomposed hexane	CO <sub>2</sub> Selectivity S <sub>CO2</sub>
< 1	59.4	2.8	3.1	0.099	0.477
2	67.2	3.6	3.2	0.102	0.527
8	71.3	19.5	23.5	0.540	0.505
11	74.1	27.0	25.4	0.682	0.535
13	77.0	31.8	31.4	0.744	0.556
15	79.9	40.7	31.7	0.903	0.564
21	82.8	41.1	37.0	0.879	0.565

**Fig. 10** Hexane dissociations by electron impact and possible byproducts



### R3 : Reactions between radicals and hexane

The gliding arc produces free electrons which dissociate the background gas. When this gas contains oxygen, the O radicals can oxidize the hexane to  $\text{CO}_2$ , CO and  $\text{H}_2\text{O}$ .

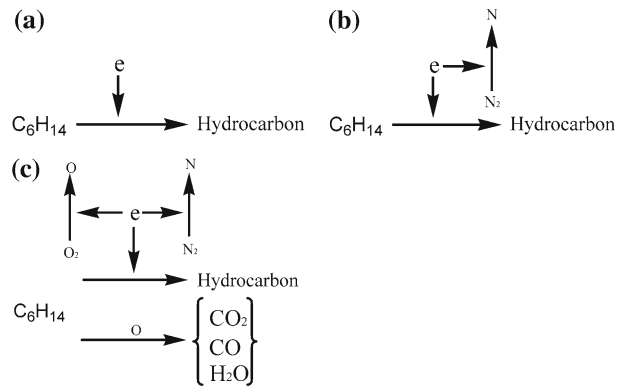
R4 : Oxidation of hydrocarbons by O radicals when the carrier gas contains oxygen.

R5 : Oxidation of  $\text{N}_2$  to  $\text{NO}_2$  by O radicals when the carrier gas contains oxygen.

Reaction R1 and R2 lead to the formation of hydrocarbon radicals. Concerning R2, the ion densities are certainly low because the mean electron energy of GA (1–5 eV) is rather lower than the ionization potential of  $\text{N}_2$  (16 eV),  $\text{O}_2$  (12 eV) and Ar (16 eV). Hence, R1 is the key channel for the production of hydrocarbon radicals. When oxygen is present in the carrier gas, these radicals lead to the production of oxides as  $\text{CO}_2$ , CO,  $\text{NO}_2$  and  $\text{H}_2\text{O}$  through R3–R5. When argon or nitrogen is the carrier gas the significant reactions are only R1 and R2. Therefore, if we ignore the reactions between ions and hexane (due to the low ion density), the hexane decomposition process under these three atmospheres can be described as shown on Fig. 11:

In argon or in nitrogen, significant amounts of gaseous C1–C4 hydrocarbons (methane  $\text{CH}_4$ , ethane  $\text{C}_2\text{H}_6$ , ethylene  $\text{C}_2\text{H}_4$  and acetylene  $\text{C}_2\text{H}_2$  mainly) are observed in the decomposition products. The electron impact is the main way to dissociate hexane (see Fig. 11a, b). When the background gas was nitrogen, a fraction of the electron energy of the discharge is consumed in the  $\text{N}_2$  dissociation. Consequently, the hexane decomposition rate and capacity in nitrogen are lower than in argon and the concentration of gaseous C1–C4 hydrocarbons is also smaller. The detection of small amounts of CO (149 ppm) and  $\text{CO}_2$  (163 ppm) among the by-products can be attributed to the existence of oxygen in the dead volume of the gliding arc reactor.

**Fig. 11** Schematic of GA hexane decomposition process in argon (a), nitrogen (b) and air (c)



When the air is chosen as the carrier gas, the electron impact also initiates the decomposition of the hexane. Furthermore, the presence of oxygen induces the oxidation of hexane to  $CO_2$ ,  $CO$  and  $H_2O$  by  $O$  radicals (see Fig. 11c). Although  $O_2$  reduces the number of electrons by attachment, and consumes a part of the electron energy in the  $O$  and  $N$  radical formations, both hexane decomposition rate and decomposition capacity are much higher when the gliding arc is working in air than when it is working in argon or in nitrogen. These observations suggest that the radical reactions and, especially the ones which involve the  $O$  radical, govern the decomposition of the hexane in a gliding arc device.

We have demonstrated that about 90% of the decomposed hexane is transformed into  $CO_2$  and  $CO$  when the oxygen concentration in the carrier gas is greater than 15%. By another hand, the  $CO_2$  selectivity increases with increasing oxygen concentration. These results indicate that oxygen promotes the conversion of hydrocarbon (including hexane) and  $CO$  to  $CO_2$ . In the meantime, when the oxygen concentration is continuously increased from 2% to 21%, the amount of  $NO_2$  in the decomposition by-products is steeply increasing when the hexane decomposition rate increases rather slowly. So, an optimum oxygen concentration remains to be found and is currently researched.

## 5 Conclusions

The experimental investigation of hexane decomposition by using a gliding arc discharge under different gas atmospheres and hexane initial concentrations has been carried out. The influence of humidity has not been taken into account. The following conclusions are obtained :

- (1) The hexane decomposition rate which can reach 94.16% when the air is chosen as the carrier gas decreases with the increase of hexane initial concentration when the decomposition capacity is continuously increasing.
- (2) In nitrogen and in argon, C1–C4 hydrocarbons (methane  $CH_4$ , ethane  $C_2H_6$ , ethylene  $C_2H_4$  and acetylene  $C_2H_2$  mainly) are the main products of hexane decomposition. In the decomposition products, neither  $NO$  nor  $NO_2$  are obtained and only small amounts of  $CO$  and  $CO_2$  are detected. In contrast,  $CO$ ,

- CO<sub>2</sub> and NO<sub>2</sub> are the predominant decomposition products when the air is chosen as the carrier gas.
- (3) The hexane decomposition rate and decomposition capacity in nitrogen are lower than in argon due to the electron energy consumption by the dissociation of nitrogen.
  - (4) Reactions between hexane and radicals, especially O radicals, are the predominant channel to the hexane decomposition process. The decomposition rate and decomposition capacity of hexane obtained in air are much higher than in nitrogen or argon.
  - (5) Increasing the oxygen concentration can raise the hexane decomposition rate and promote the conversion of hydrocarbon and CO to CO<sub>2</sub>, but also leads to a steep increase of NO<sub>2</sub>.

**Acknowledgments** Financial support from National Nature Science Foundation (N50476058) and Science and Technology Bureau of Zhejiang Province is much acknowledged. The support from PRA (Program Sino-French of Advanced Research) was provided by the Institute for Thermal Power Engineering (Zhejiang University, China) and CORIA (France). The programme is authorized by the Ministry of Science and Technology of PRC and the Ministry of Science and Technology of France. The authors gratefully acknowledge the technical assistance for the experimental apparatus afforded by CORIA.

## References

1. Schutze A, Jeong JY, Babayan SE, Park J, Selwyn GS, Hicks RF (1998) *IEEE Trans Plasma Sci* 26:1685
2. Nichipor H, Dashouk E, Chmielewski AG, Zimek Z, Bulka S (2000) *Radiat Phys Chem* 57:519
3. Yamamoto T (1997) *J Electrostat* 42:227
4. Kalra CS, Gutsol AF, Fridman AA (2005) *IEEE Trans Plasma Sci* 33:32
5. Fridman A, Nester S, Kennedy A, Saveliev A (1999) *Energy Combust Sci* 25:211
6. Paulmier T, Fulcheri L (2005) *Chem Eng J* 106:59
7. Pospisil M, Viden I, Simek M, Pekarek S (2001) *Int J Vehicle Design* 27:306
8. Delair L, Brisset JL, Chéron BG (2001) *High Temp Mat Process* 5:381
9. Mutaf-Yardimci O, Saveliev AV, Fridman AA, Kennedy LA (2000). *J Appl Phys* 87:1632
10. Pellerin S, Cormier JM, Richard F, Musiol K, Chapelle J (1999) *J Phys D: Appl Phys* 32:891
11. Richard F, Cormier JM, Pellerin S, Chapelle J (1996) *J Appl Phys* 79:2245
12. Czernichowski A (1994) *Pure & Appl Chem* 66:1301
13. Krawczyk K, Ulejczyk B (2003) *Plasma Chem Plasma Process* 23:265
14. Krawczyk K, Ulejczyk B (2004) *Plasma Chem Plasma Process* 24:155
15. Czernichowski A, Ranaivosoloarimanana A (1996) *Chemtech* 26:45
16. Mok YS, Nam I (2002) *Chem Eng J* 85:87
17. Futamura S, Zhang AH, Yamamoto T (1997) *J Electrostat* 42:51
18. Kohno H, Berezin AA, Chang JS, Yamamoto T, Shibuya A, Honda S (1998) *IEEE Trans Plasma Sci* 34:953